

A novel water-soluble near-infrared glucose-conjugated porphyrin: synthesis, properties and its optical imaging effect

Feng Lv, Xujun He, Li Lu, Li Wu and Tianjun Liu*[◇]

Institute of Biomedical Engineering, Chinese Academy of Medical Sciences & Peking Union Medical College, The Tianjin Key Laboratory of Biomaterial Research, Tianjin 300192, PR China

Received 22 March 2011

Accepted 5 May 2011

ABSTRACT: A simple novel near-infrared water-soluble glucose-conjugated porphyrin, 5,15-bis-[(trimethylsilyl)ethynyl]-10,20-bis[4- β -D-glucopyranosyl]phenylporphyrin, with good optical stability and high emission ability in near-infrared region, was synthesized. And Optical Imaging *in vivo* with this compound as probe was performed on liver tumor-bearing nude mice. The result shows that this glucose-conjugated porphyrin could display information *in vivo* more than 1 cm in depth, which implies its potential application as optical probe in cancer diagnosis.

KEYWORDS: near infrared fluorescence, porphyrin, glucose conjugated, optical imaging.

INTRODUCTION

Near-infrared (NIR) fluorescence imaging can provide information *in vivo* in deep tissues and organs owing to its specific advantages [1, 2], such as low cost, high sensitivity and being environmentally friendly, *etc.* The drawback is not so large difference among tissues. In order to improve sensitivity and accuracy, molecular probe with near-infrared fluorescence imaging ability should be used. Up to now, several kinds of optical probe with emission in NIR region have been developed [3–5], including phthalocyanines, dipyrro BF₂ chelate, quantum dots, rare earth materials [1, 2, 6, 7]. As optical probe several properties are required including light transmission in depth, the luminescence quantum yield, good biocompatibility as well as targeting ability, so a great scientific effort has been focused on the development of near-infrared fluorescence imaging [3–5].

Porphyrins and their derivatives have extended π -conjugated electronic structure, large visible to NIR absorption molar extinction constant, acceptable fluorescent quantum yields, and good biocompatibility. Their

luminescence efficiency, emission wavelength as well as the singlet and triplet state characteristics could be tuned by peripheral substituents and the porphyrin inner metal. All these characteristics of porphyrin above made the porphyrin system have wide application in biomedical fields including photodynamic therapy (PDT) sensitizer [8], fluorescent imaging probe [9–11], as well as oxygen carriers [12], *etc.* NIR emission or absorption as the result of low-energy electron jump between the front orbitals, only occurs in a large electronic delocalization system, so to develop NIR optical probe need to construct a large electron delocalization system. Although porphyrin monomer possesses large planar electronic delocalization ability, its absorption ability in NIR region is not so high. Expanded porphyrin [13, 14] or porphyrin dimer, conjugated oligomer [15, 16] *etc.*, have NIR absorption and emission ability but their bulky size cause problem in solubility and membrane permeability. Approaches like introducing long alkyl chain to increase the hydrophobic solubility in electronic materials fields, does not meet the water solubility require in biomedical fields. Although microspheric approach reported by Theirin [17] can be an alternative way for hydrophobic NIR porphyrin probe, water-soluble porphyrin NIR probe is desired in optical imaging. However, to the best of our knowledge, up to now we have not found any report of water-soluble NIR

[◇]SPP full member in good standing

*Correspondence to: Tianjun Liu, email: liutianjun@hotmail.com, tel: +86 22-87893236, fax: +86 22-87893236

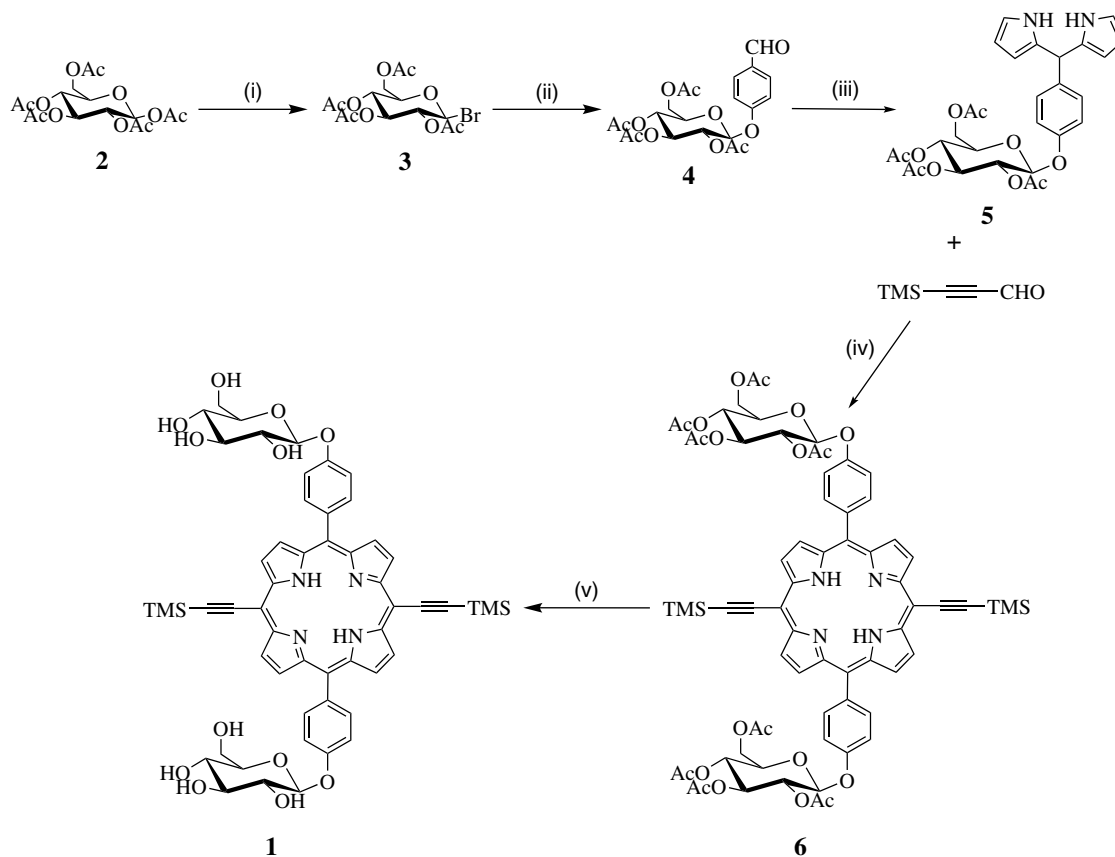
porphyrin compounds *in vivo* optical imaging. Many water-soluble porphyrin reported was achieved by periphery introducing charge-bearing moieties like ammonium, sulfonate, and carboxylate as well as neutral polar moieties like PEG, saccharide, *etc.* [18, 19]. Consideration of biocompatibility and targeting effect, conjugated with saccharide is more advantageous, because saccharide modification can not only improve the substrate water solubility and biocompatibility, but also may increase tumor targeting function, successful examples are imaging probes and PDT sensitizer [20, 21]. In NIR optical imaging field, saccharide conjugation of porphyrin with NIR fluorescence has not been reported before. In this paper, a simple approach to construct porphyrin-based near-infrared fluorescent probe, with glucose-conjugation to enhance water solubility, alkyne moiety to extend electronic delocalization to NIR region, with NIR Optical imaging *in vivo*, was reported.

RESULTS AND DISCUSSION

5,15-Bis[(trimethylsilyl)ethynyl]-10,20-bis[4- β -D-glucopyranosyl]phenyl]porphyrin (**1**) was synthesized in four steps shown in Scheme 1. 4-(2,3,4,6-tetra-O-acetyl- β -D-glucopyranosyl) benzaldehyde (**4**) was achieved in 30% yield in a routine two steps from 1,2,3,4,6-penta-O-acetyl- β -D-glucopyranose (**2**) and 4-hydroxybenzaldehyde

by bromination and condensation. Condensation compound **4** with pyrrole according to Lindsey method with TFA as catalyst affords corresponding 4-(2,3,4,6-tetra-O-acetyl- β -D-glucopyranosyl)-2,2'-dipyrrolyl-methyl benzene (**5**), which was purified by flash column chromatography (ethyl acetate/petroleum ether = 1:2 v/v) as white solid in 68% yield. Corresponding porphyrin was obtained by condensation compound **5** and 3-(trimethylsilyl)propynal and then oxidation by DDQ affords compound **6**, 5,15-bis[(trimethylsilyl)ethynyl]-10,20-bis[4-(2,3,4,6-tetra-O-acetyl- β -D-glucopyranosyl)phenyl]porphyrin, purified by flash column chromatography as purple solid in 51.2% yield. Deprotection of **6** in dry MeOH and NaOMe then recrystallization from water and acetone, gives the water soluble target compound (**1**) as a greenish purple solid in 89% yield.

The structures of products were characterized by NMR spectroscopy and MS. For target compound **1**, broad bands at 3–4 ppm in ^1H NMR indicate the saccharide moiety and low fields in 7.50, 8.14, 8.90, 9.65 ppm indicate the aromatic proton at phenyl and pyrrolyl moieties, *etc.*, peak at -2.433 ppm, a characteristic porphyrin signal of NH proton indicated a pure porphyrin compound. High resolution MALDI-TOF-HRMS confirmed the target compound. The optical characters of target compound were evaluated by UV-vis and fluorescence spectrum in Fig. 1. The spectrum in DMSO is well-defined,



Scheme 1. Synthetic route of glucose-conjugated porphyrin **1**. (i) CH_2Cl_2 , HBr/HOAc , 0°C ; (ii) CH_2Cl_2 , 4-hydroxybenzaldehyde, NaOH , PTC , rt; (iii) TFA, pyrrole, rt; (iv) TFA, CH_2Cl_2 , DDQ, N_2 , rt; (v) MeOH, NaOMe, rt

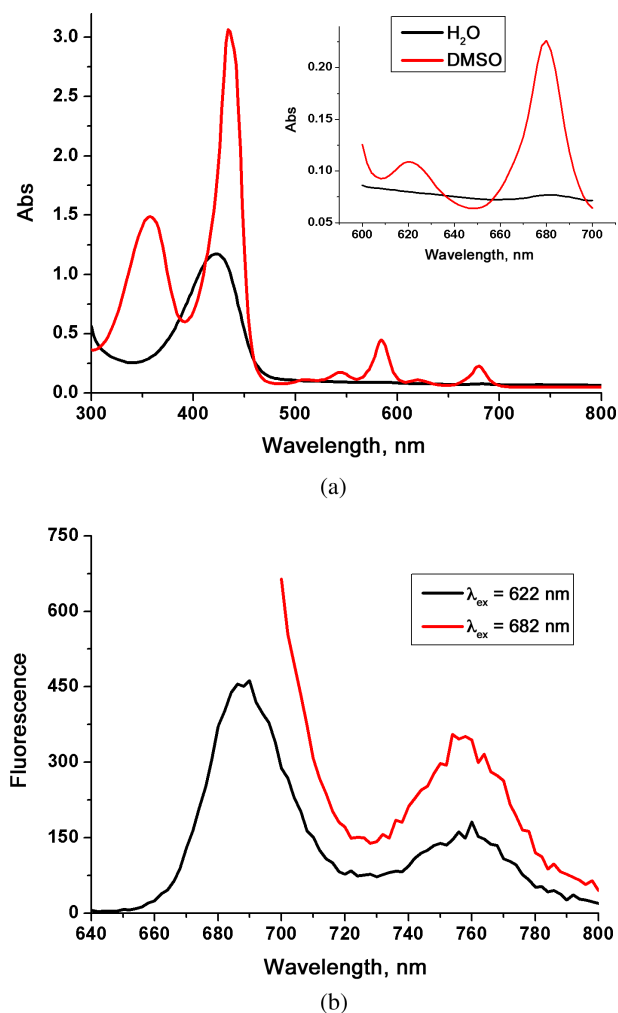


Fig. 1. Optical spectrum of glucose-conjugated porphyrin in different condition. (a) UV-vis spectrum of glucose-conjugated porphyrin in different solvents (2×10^{-5} M; red line: UV-vis spectrum in DMSO; black line: UV spectrum in H_2O ; inset: UV-vis spectrum from 600–700 nm). (b) Fluorescence spectrum of glucose conjugated porphyrin at different exciting wavelength (2×10^{-5} M; black line: fluorescence spectrum in DMSO at exciting wavelength of 622 nm; red line: fluorescence spectrum in DMSO at exciting wavelength of 682 nm)

characteristic bands are seen at 360, 435, 520, 580, 622 and 682 nm respectively, indicating no intermolecular aggregation. However, the absorption spectrum of glucose conjugated porphyrin in water differs remarkably from that in DMSO. Intensity of absorption peak in water is much lower than that in DMSO, indicating aggregation due to cofacial arrangement of porphyrin [22, 23]. The Soret band is slightly shifted to shorter wavelength (420 nm), whereas the Q-band was little shown in wavelength of 600–800 nm. Consistent with absorption, weak fluorescence signal indicates glucose conjugated porphyrin aggregation in water again, while in DMSO (Fig. 2) a strong fluorescence peak at 685 nm and 760 nm with exciting wavelength at 622 nm and 682 nm indicates disperse state. With 5,10,15,20-tetraphenylporphyrin as reference sample, fluorescent quantum yield of target

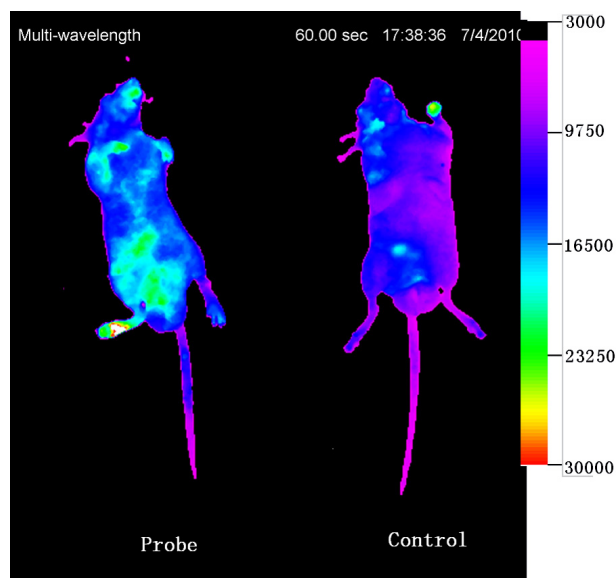


Fig. 2. Optical imaging *in vivo* with glucose-conjugated porphyrin as probe, liver tumor-bearing nude mice as model (injected with 200 μ l of 2×10^{-4} M with an exposure time of 1 min (filters: excitation 625 nm, emission 700 nm))

compound **1** is 5% in DMSO. Either in DMSO or in water solution, both the excitation and emission region falls into the tissue transparency window NIR region, which indicates this porphyrin compound is suitable for NIR imaging *in vivo*. Although aggregation of compound **1** in water induces its low fluorescent ability, however the following fluorescent imaging *in vivo* confirmed this does not limit its application as fluorescence probe *in vivo*. A reasonable interpretation maybe: after administer to blood, aggregation of compound **1** will be broken into dispersed single molecule, which maybe intercalated into the constrained environment of bio-macromolecules. This constrained state reduces the nonradiation energy-loss path, such as rotation and vibration processes, then results in the illumination path enhancing. The net effect exhibits as emission enhancement in biological system.

The NIR fluorescent imaging was conducted with liver tumor-bearing athymic nude mice as animal model. Among two groups of model mice, one group was injected 200 μ l of compound **1** at 2×10^{-4} M *via* tail vein, and another group was injected equal amount of saline as control. The *in vivo* imaging at 12 h post injections were acquired respectively using a Kodak *In-Vivo* FX Professional Imaging System equipped with fluorescent filter sets (excitation/emission, 625/700 nm) near optimal wavelength. Figure 2 shows the real-time images of near infrared fluorescence agent in the tumor-bearing mice. A strong luminescence signal was detected in mice body at 12 h post injections, especially in liver and kidney tissue, whereas weak luminescence signal was observed in the control group. These results indicate that *in vivo* glucose-conjugated porphyrin is emissive and suitable as NIR fluorescent imaging probe. Besides the left armpit of model mice where tumor was planted, normal liver and kidney

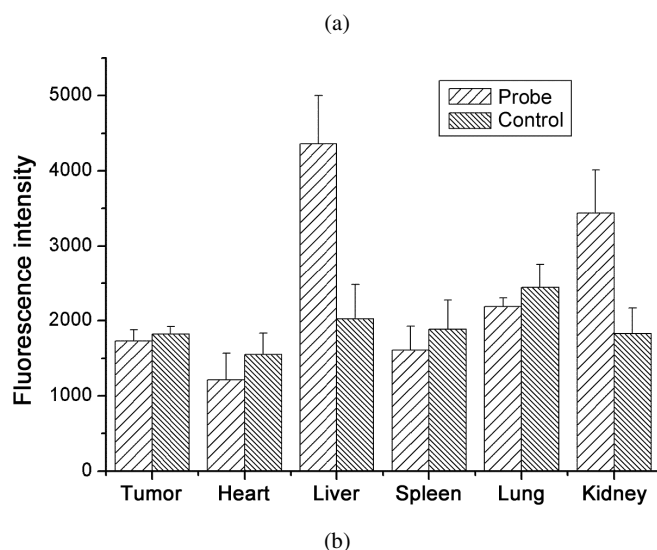
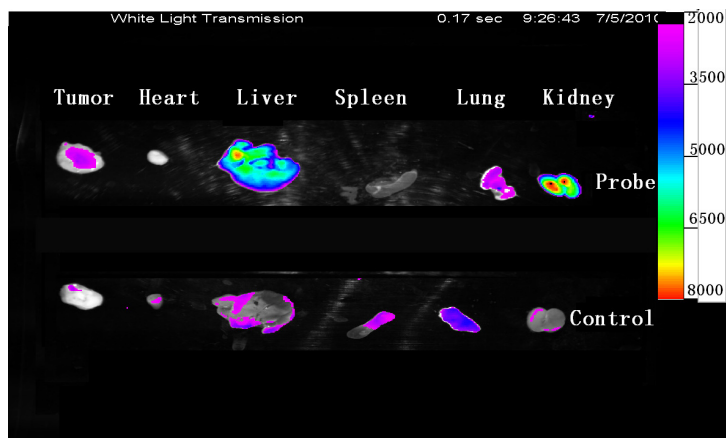


Fig. 3. Distribution and fluorescent intensity of dissected organs. (a) *Ex vivo* imaging with an exposure time of 1 min (filters: excitation 625 nm, emission 700 nm). (b) Quantitative analysis

also give apparent emission signal, which indicates glucose conjugation is short of targeting effect.

To further investigate distribution of the probe in various organs, *ex vivo* fluorescence imaging of organs was recorded. At 12 h time-point after probe injection, the animals were sacrificed immediately. The kidney, heart, liver, lung, spleen, muscle and tumor were harvested and subjected to the imager, then quantitative analysis was conducted using the Kodak Image Analysis Software. The fluorescent images of dissected mice organs show the strongest fluorescent signal from the liver and kidney, while a little in the heart, lung and muscle. This is in accord with the imaging *in vivo*, and the fluorescent intensity of the sample group was about 2-fold higher than that of control group in liver and kidney. Results above indicate that compound **1**, actually as optical probe *in vivo*, can penetrate more than 1 cm in depth (based upon the liver, heart depth in mice body). After 12 h circulation the probe was mainly accumulated in two main metabolism organs including liver and kidney.

In summary, an easy condensation methodology to access high yields simple water soluble NIR porphyrin has been described. Optical imaging *in vivo* on liver tumor-bearing nude mice shows that glucose-conjugated porphyrin can work as optical probe well. Probe reported here is very small in size compared with other NIR porphyrin-based probes and so it is suitable to transport across cellular membrane, and the fact that after 12 h circulation mainly remained in kidney and liver indicates that the probe have a suitable circulation retained time in body for imaging. Small modifications to its structure can enhance its targeting and extend its emission region, because alkyne is a versatile functional moiety to take place click or coupling reaction. Porphyrin's good biocompatibility combined with alkyne transformation characteristics makes this system an attractive platform for development of optical probe for future imaging *in vivo*.

EXPERIMENTAL

General methods and materials

The ^1H NMR spectra were recorded on Varian Mercury at 300 MHz using CDCl_3 or DMSO-d_6 as solvent and TMS as internal reference. MS and HRMS were recorded on Finnigan Trace DSQ and Bruker autofle III SmartBeam MALDI-TOF instrument. The UV-vis and fluorescence spectra were recorded on a ThermoFisher scientific Varioskan TM Flash multimode microplate spectra photometer. All purchased materials were used without further purification.

4-(2,3,4,6-tetra-O-acetyl- β -D-glucopyranosyl)benzaldehyde (4). To a stirring solution of compound **2** (24 g) in CH_2Cl_2 (200 mL) was added HBr/HOAc (100 mL, 33%) solution at 0°C . The resulting solution was stirred for 7 h until **2** completely disappeared monitored by TLC. The solution was neutralized with saturated NaHCO_3 aqueous solution. The organic layer was separated, washed with water and combined, then a mixture solution of 4-hydroxybenzaldehyde in 100 mL CH_2Cl_2 , 160 mL 5% NaOH aqueous solution, and tetrabutyl ammonium fluoride were added. The resulting solution was stirred for 48 h at room temperature. Then the reaction was quenched and concentrated in vacuum. The concentrate was purified by silica flash column chromatography (ethyl acetate:petroleum = 3:7 in v/v) to give the desired white crystalloid compound (**4**). Yield 8.3 g (30%), mp $129\text{--}131^\circ\text{C}$. ESI-MS: m/z ($\text{C}_{21}\text{H}_{24}\text{O}_{11}$) 475.21 (calcd. for $[\text{M} + \text{Na}]^+$ 475.12). ^1H NMR (CDCl_3 , 300 MHz): δ , ppm 9.932 (s, 1H), 7.850 (d, 2H, $J = 1.8$ Hz), 7.095 (d, 2H, $J = 1.8$ Hz), 5.281–5.334 (m, 2H), 5.153–5.232 (m, 2H),

4.297 (dd, 1H, $J = 5.1$ Hz, $J = 6.9$ Hz), 4.183 (dd, 1H, $J = 2.4$ Hz, $J = 9.9$ Hz), 3.935 (m, 1H), 2.165 (s, 3H, CH₃), 2.107 (s, 3H, CH₃), 2.070 (s, 3H, CH₃), 2.050 (s, 3H, CH₃).

4-(2,3,4,6-tetra-O-acetyl-β-D-glucopyranosyl)phenyl-2,2'-dipyrrromethane (5). TFA (76 μL) was added to a stirring solution of compound **4** (4.5 g, 20 mmol) in pyrrole (20 mL) solution. Then the resulting solution was stirred for 2 h at the room temperature. The solution was concentrated under reduced pressure and purified by flash column chromatography (ethyl acetate:petroleum = 1:2 in v/v) to give the desired white solid compound (**5**). Yield 3.8 g (68%), mp 146–148 °C. ESI-MS: m/z (C₂₉H₃₂N₂O₁₀) 569.00 (calcd. for [M + H]⁺ 569.21). ¹H NMR (CDCl₃, 300 MHz): TM, ppm 7.938 (s, 2H), 7.115 (d, 2H, $J = 4.5$ Hz), 6.903 (d, 2H, $J = 2.1$ Hz), 6.668 (dd, 2H, $J = 1.5$ Hz, $J = 2.7$ Hz), 6.129 (dd, 2H, $J = 2.4$ Hz, $J = 3.3$ Hz), 5.869 (m, 2H), 5.415 (s, 1H), 5.191 (m, 1H), 5.051 (dd, 1H, $J = 2.7$ Hz), 4.268 (dd, 2H, $J = 5.4$ Hz, $J = 6.9$ Hz), 4.116 (m, 1H), 3.831 (m, 1H), 2.088 (m, 12H).

5,15-bis[(trimethylsilyl)ethynyl]-10,20-bis[4-(2,3,4,6-tetra-O-acetyl-β-D-glucopyranosyl)phenyl]porphyrin (6). TFA (8 μL) was added to a stirring solution of compound **5** (113.6 mg, 0.2 mmol) and 3-(trimethylsilyl)propynal (25.2 mg, 0.2 mmol) in CH₂Cl₂ (20 mL) under N₂ for 30 min. Then DDQ (90 mg) was added, and stirred for 2 h at room temperature. The reaction was quenched with 20 μL triethyl amine, and the mixture was concentrated under reduced pressure and purified by flash column chromatography (ethyl acetate:petroleum = 1:1 in v/v) to give a greenish purple solid **6**. Yield 69 mg (51.2%), mp > 300 °C. MALDI-TOF-HRMS: m/z (C₇₀H₇₄N₄O₂₀Si₂) 1347.4527 (calcd. for [M + H]⁺ 1347.4508). ¹H NMR (CDCl₃, 300 MHz): TM, ppm 9.587 (d, 4H, $J = 4.5$ Hz), 8.806 (d, 4H, $J = 4.5$ Hz), 8.102 (d, 4H, $J = 8.1$ Hz), 7.405 (d, 4H, $J = 8.4$ Hz), 5.441–5.521 (m, 6H), 5.303–5.359 (m, 2H), 4.449 (dd, 2H, $J = 5.4$ Hz, 6.9 Hz), 4.331 (dd, 2H, $J = 2.4$ Hz, 9.9 Hz), 4.058–4.116 (m, 2H), 2.251 (s, 6H, 2CH₃), 2.162 (s, 6H, 2CH₃), 2.124–2.137 (m, 12H, 4CH₃), 0.620 (s, 18H, 6CH₃).

5,15-bis[(trimethylsilyl)ethynyl]-10,20-bis[4-β-D-glucopyranosyl]phenylporphyrin (1). Compound (**6**) (60 mg, 0.044 mmol) was suspended in dry MeOH (10 mL). NaOMe (300 μL, 1.0 M) was added and the solution was stirred for 4–5 h at room temperature. Cationic ion exchanger 001 × 7 was added to neutralize the solution. The ion exchanger was then filtered off and the solvent was evaporated to dry, then the residue was dissolved in a minimal amount of water, and acetone was added to recrystallize the product, the solid was filtered, and dissolved again in a minimal amount of water, recrystallized by acetone and collected after filtration. Finally the water soluble target compound (**1**) was obtained as a greenish purple solid **1**. Yield 41 mg (89%), mp > 300 °C. MALDI-TOF-HRMS: m/z [M + H]⁺ (C₅₄H₅₈N₄O₁₂Si₂) 1011.3658 (calcd. for [M + H]⁺ 1011.3663). ¹H NMR (DMSO-d₆, 300 MHz): TM, ppm 9.651 (d, 4H, $J = 4.7$ Hz), 8.909

(d, 4H, $J = 4.6$ Hz), 8.139 (d, 4H, $J = 8.4$ Hz), 7.507 (d, 4H, $J = 8.4$ Hz), 5.753 (s, 8H), 0.011 (s, 18H), -2.45 (2H -NH).

In vivo imaging and distribution of glucose conjugated alkyl porphyrin

Athymic nude mice (seven weeks old, 20–25 g) were used. All the animal experiments were performed in compliance with the Guiding Principles for the Care and Use of Laboratory Animals, Peking Union Medical College, China. Animals can access free to food and water. Tumor-bearing mice were prepared by injecting a suspension of 1 × 10⁶ liver tumor cells in physiological saline (100 μL) into the subcutaneous left flank. Tumors develop within a period of 1 week. Athymic nude mice were randomly assigned to perform as follows: glucose conjugated alkyl porphyrin, control group (n = 6 for each group). In experimental group, near infrared fluorescence agent was injected into the tail vein of the liver tumor-bearing mice at 200 μL of 2 × 10⁻⁴ M. Images were taken using a Kodak Image Station *in vivo* FX (filters: excitation 625 m, emission 700 nm) with an exposure time of 1 min. At the end of the imaging, anesthetized mice were sacrificed and images of organs were made to evaluate the distribution of near infrared fluorescence agent. Fluorescence image of organ was analyzed using the Kodak Image Analysis Software.

Acknowledgements

This work is supported by the National Basic Research Program of China (No. 2006CB705703) and the PhD Programs Foundation of Ministry of Education of China (Nos. 20101106120052, 20070023020).

Supporting information

¹H NMR and MS data of compound **4**, **5**, **6** and **1** are given in the supplementary material. This material is available free of charge *via* the Internet at <http://www.worldscinet.com/jpp/jpp.shtml>.

REFERENCES

1. Rao JH, Dragulescu A and Yao HQ. *Curr. Opin. Biotechnol.* 2007; **18**: 17–25.
2. Hilderbrand SA and Weissleder R. *Curr. Opin. Chem. Biol.* 2010; **14**: 71–79.
3. Kobayashi H, Ogawa M, Alford R, Choyke PL and Urano Y. *Chem. Rev.* 2010; **110**: 2620–2640.
4. Pham W, Cassell L, Gillman A, Koktysh D and Gore JC. *Chem. Commun.* 2008; 1895–1897.
5. Escobedo JO, Rusin O, Lim S and Strongin RM. *Curr. Opin. Chem. Biol.* 2010; **4**: 64–70.
6. Michalet X, Pinaud F, Bentolila LA, Tsay JM, Doose S, Li JJ, Sundaresan G, Wu AM, Gambhir SS and Weiss S. *Science.* 2005; **307**: 538–544.

7. Xiong LQ, Chen ZG, Yu MX, Li FY, Liu C and Huang CH. *Biomaterials* 2009; **30**: 5592–5600.
8. Moore CM, Pendse D and Emberton M. *Nat. Clin. Pract. Urol.* 2009; **6**: 18–30.
9. Chiang CK, Huang CC, Liu CW and Chang HT. *Anal. Chem.* 2008; **80**: 3716–3721.
10. Christian NA, Benencia F, Milone MC, Li G, Frail PR, Therien MJ, Coukos G and Hammer DA. *Mol. Imag. Biol.* 2009; **11**: 167–177.
11. Wu D, Descalzo AB, Weik F, Emmerling F, Shen Z, You XZ and Rurack K. *Angew. Chem., Int. Ed.* 2007; **47**: 193–197.
12. Tsuchida E, Sou K, Nakagawa A, Sakai H, Komatsu T and Kobayashi K. *Bioconjugate Chem.* 2009; **20**: 1419–1440.
13. Zhu XJ, Fu ST, Wong WK, Guo JP and Wong WY. *Angew. Chem., Int. Ed.* 2006; **45**: 3150–3154.
14. Zhu XJ, Fu ST, Wong WK and Wong WY. *Tetrahedron Lett.* 2008; **49**: 1843–1846.
15. Thorley KJ, Hales JM, Anderson HL and Perry JW. *Angew. Chem.* 2008; **120**: 7203–7206.
16. Wilson GS and Anderson HL. *Chem. Commun.* 1999; 1539–1540.
17. Ghoroghchian TP, Frail PR, Susumu K, Blessington D, Brannan AK, Bates FS, Chance B, Hammer DA and Therien MJ. *PNAS* 2005; **102**: 2922–2927.
18. Kim WJ, Kang MS, Kim HK, Kim Y, Chang T, Ohulchanskyy T, Prasad PN and Lee K. *J. Nanosci. Nanotechnol.* 2009; **9**: 7130–7135.
19. Cao Y, Gill AF and Dixon DW. *Tetrahedron Lett.* 2009; **50**: 4358–4360.
20. Aksenova AA, Sebyakin YL and Mironov AF. *Russ. J. Bioorg. Chem.* 2003; **29**: 201–219.
21. Chen X, Hui L, Foster DA and Drain CM. *Biochemistry* 2004; **43**: 10918–10929.
22. Kroon JM, Sudhoelter EJ, Schenning AP and Nolte RJ. *Langmuir* 1995; **11**: 214–220.
23. Hoeben FJM, Wolfs M, Zhang J, Feyter SD, Leclère P, Schenning AP and Meijer EW. *J. Am. Chem. Soc.* 2007; **129**: 9819–9828.